7264 *Biochemistry* **2010,** *49,* 7264–7271
DOI: 10.1021/bi100831w

BIOCHEMISTRY
including biophysical chemistry & molecular biology
Article

Fluoride-Dependent Conversion of Organic Compounds Mediated by Manganese Peroxidases in the Absence of Mn^{2+} Ions[†]

Lidan Ye,[‡] Dieter Spiteller,[§] René Ullrich,[∥] Wilhelm Boland,[§] Jörg Nüske,[‡] and Gabriele Diekert*[,‡]

[‡]*Department of Applied and Ecological Microbiology, Institute of Microbiology, Friedrich Schiller University, 07743 Jena, Germany,* [§]*Department of Bioorganic Chemistry, Max Planck Institute for Chemical Ecology, 07745 Jena, Germany, and* [∥]*Department of Environmental Biotechnology, International Graduate School, 02763 Zittau, Germany*

Received May 25, 2010; Revised Manuscript Received July 26, 2010

ABSTRACT: Manganese peroxidase generally mediates the oxidation of Mn^{2+} to Mn^{3+} with H_2O_2 as an oxidant. Several manganese peroxidases purified from different lignin-degrading fungi were found to mediate a fluoride-dependent conversion of organic substrates such as monochlorodimedone or 2,6-dimethoxyphenol in the absence of manganese ions. Using the manganese peroxidase MnP-1 from *Bjerkandera adusta* strain Ud1, these fluoride-dependent reactions were studied with respect to different substrates converted, reaction products, and kinetic properties to shed some light on the reaction mechanism of manganese peroxidase. The analysis of the reaction products formed from monochlorodimedone and 2,6-dimethoxyphenol showed that the substrates were oxidized rather than fluorinated. The addition of fluoride to MnP-1 resulted in altered absorption spectra, indicating a coordinative binding of fluoride or HF to the heme iron; the fluoride:heme stoichiometry was determined to be 1:1 and the K_D value to be ~2.5 mM at pH 3.4. The high K_D value indicates weak binding of fluoride to the heme. Fluoride appeared to act as a partially competitive inhibitor with respect to hydrogen peroxide for binding to the heme as the sixth ligand. From the findings, a putative model for the fluoride-dependent reaction was developed. The data were interpreted to indicate that changes of the reaction center of manganese peroxidase as, for example, caused by fluoride binding may lead to the oxidation of organic compounds in the absence of manganese by opening a long-range electron transfer pathway.

MnPs[1] are excreted by many white rot basidiomycetes such as *Bjerkandera adusta* and, together with other heme peroxidases such as lignin peroxidases and versatile peroxidases, are responsible for the decomposition of lignin. The manganese peroxidase mediates the oxidation of Mn^{2+} to Mn^{3+} with H_2O_2 as an oxidant. During the catalytic cycle, H_2O_2 reacts with the resting enzyme. After release of H_2O, compound I is formed as an oxidation product. Compound I is reduced in two steps of a one-electron transfer reaction via compound II to the resting enzyme; the electron donor for the reduction steps is Mn^{2+} (Figure 1) (*1*). The reaction product Mn^{3+} oxidizes organic compounds such as lignin or phenols in a protein-independent abiotic reaction (*2*, *3*). A manganese-independent oxidation of organic compounds by MnPs was not observed, except for an unusual manganese peroxidase that in fact exhibited characteristics of a versatile peroxidase (VP) with respect to the substrates oxidized in the absence of manganese ions. This enzyme mainly differs from the VP in its inability to catalyze the Mn-independent oxidation of veratryl alcohol (*4*). In addition, transient-state studies on MnPs have shown that compound I can oxidize Mn^{2+} as well as some phenolic compounds; however, only Mn^{2+} was able to efficiently reduce compound II and to close the catalytic cycle (*5*). These results point out the crucial role Mn^{2+} plays in the catalytic cycle of MnPs. A manganese-independent oxidation of veratryl alcohol mediated by manganese peroxidase was earlier only observed for a MnP mutant (*6*). This modified MnP was found to adopt characteristics of the versatile peroxidases; the modification enabled the enzyme to oxidize veratryl alcohol in the absence of Mn^{2+} ions via a long-range electron transfer pathway. Long-range electron transfer pathways have been described for lignin peroxidase and versatile peroxidase (*7*, *8*) and were also reported to be involved in other important biological processes, e.g., photosynthesis and respiration (*9*). Here, we describe for the first time a Mn^{2+}-independent oxidation of organic substrates

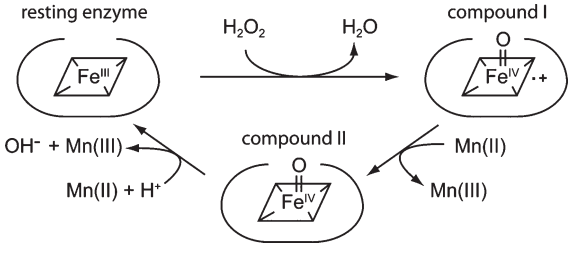

FIGURE 1: Simplified scheme of the Mn^{2+}-dependent catalytic cycle of manganese peroxidase.

[†]This work was supported by a grant from the Deutsche Forschungsgemeinschaft (DFG) within the ILRS graduate school in Jena. D.S. is grateful for the financial support by DFG within the Emmy Noether Programme (SP1106/3-1).

*To whom correspondence should be addressed: Institute of Microbiology, Friedrich Schiller University, Philosophenweg 12, 07743 Jena, Germany. Phone: 0049-3641-949300. Fax: 0049-3641-949302. E-mail: gabriele.diekert@uni-jena.de.

[1]Abbreviations: MnP, manganese peroxidase; LiP, lignin peroxidase; VP, versatile peroxidase; ABTS, 2,2′-azinobis(3-ethyl-benzthiazoline-6-sulfonic acid); MCD, monochlorodimedone; 2,6-DMP, 2,6-dimethoxyphenol; VA, veratryl alcohol; SDS−PAGE, sodium dodecyl sulfate−polyacrylamide gel electrophoresis.

 Published on Web 07/28/2010

catalyzed by heme-containing MnPs exclusively in the presence of fluoride. Fluoride is known to be an inactivator or inhibitor for numerous enzymes (*10*−*12*). In heme-containing peroxidases, fluoride binds to the heme iron as a distal ligand and may cause conformational changes in the protein structure by forming hydrogen bonds to amino acid side chains (*13*). For cytochrome *c* peroxidase, structural perturbations were caused by fluoride binding to the heme iron (*14*). The impact of binding of fluoride to MnP on the oxidation of organic substrates and the possible involvement of a conformational change of the protein is discussed.

MATERIALS AND METHODS

Materials. The fungal strains *Phlebia* spp. (formerly *Nematoloma frowardi*) b19 (DSM 11237) and *Clitocybula dusenii* b11 (DSM 11238) were isolated from decaying wood in Bariloche, Argentina (*15*). *B. adusta* strain Ud1 (DSM 23426) was isolated from the fruiting body on a Beech stump (*Fagus sylvatica*) in Hainich National Park (Germany). *Pleurotus eryngii* (DSM 9619) was obtained from the German Collection of Microorganisms and Cell Cultures (DSMZ, Braunschweig, Germany). All chemicals used were of the highest available purity and were purchased from Sigma-Aldrich (Steinheim, Germany), Merck (Darmstadt, Germany), Roche (Mannheim, Germany), or Roth (Karlsruhe, Germany).

Purification of MnP-1 from B. adusta Strain Ud1. The manganese peroxidase (MnP-1) of *B. adusta* strain Ud1 was purified in 10 mM acetate buffer (pH 5.6) using fast performance liquid chromatography (FPLC) essentially according to the work of Ullrich et al. (*16*) with a few modifications. After anion exchange chromatography performed on a Q-Sepharose column (1.6 cm × 10 cm) and a subsequent Mono Q column (0.5 cm × 5 cm), an additional Mono Q column was used to separate the two MnP isoenzymes. These isoenzymes were designated MnP-1 and MnP-2 according to their order of elution. MnP-1, which was used for the studies, was eluted with an isocratic step of 0.1 M NaCl in acetate buffer. For further purification, the active fractions were pooled and applied to a Phenyl-Superose HR column (0.5 cm × 5 cm), and the enzyme was eluted at a $(NH_4)_2SO_4$ concentration of approximately 0.3 M with a >99% apparent homogeneity as indicated by the SDS−PAGE gel. The MnPs from other fungal species were purified in a similar way. Chromatography media and instruments were from Pharmacia Biotech (Uppsala, Sweden).

The protein concentration was determined according to the method of Bradford (*17*) using Roti-Nanoquant (Roth) as a reagent according to the manufacturer's instructions.

Enzyme Assays. Manganese peroxidase activity was assayed photometrically at pH 4.5 by assessing the formation of the Mn^{3+}−malonate complex (Mn^{3+}−malonate ε_{270} = 11.59 mM^{-1} cm^{-1}) (*18*). MnP-1-mediated conversion of 0.1 mM monochlorodimedone (monochlorodimedone ε_{278} = 12.2 mM^{-1} cm^{-1}), 1 mM 2,6-dimethoxyphenol (3,3′,5,5′-tetramethoxy-4,4′-diphenoquinone ε_{469} = 27.5 mM^{-1} cm^{-1}), 1 mM guaiacol (guaiacol tetramer ε_{470} = 26.6 mM^{-1} cm^{-1}), 0.3 mM ABTS ($ABTS^+$ ε_{420} = 36 mM^{-1} cm^{-1}), or 4 mM veratryl alcohol (veratraldehyde ε_{310} = 9.3 mM^{-1} cm^{-1}) was followed photometrically in 100 mM citrate/phosphate buffer (pH 2.8) in the presence of 20 mM NaF and 1 mM H_2O_2.

If not otherwise stated, the MnP-1-mediated fluoride-dependent reactions were performed in 100 mM citrate/phosphate buffer (pH 2.8) in the presence of 20 mM NaF and 1 mM H_2O_2, whereas Mn^{2+} oxidation was assessed in 50 mM malonate buffer (pH 4.5) containing 0.5 mM Mn^{2+} and 0.2 mM H_2O_2.

Using the spectrophotometric assays described above, the pH optima for the fluoride-dependent reactions with monochlorodimedone (0.1 mM) or 2,6-dimethoxyphenol (1.0 mM) as substrates were determined in the absence of Mn^{2+} in 100 mM tartrate buffer at pH values from 2.0 to 8.0 in the presence of 10 mM NaF. H_2O_2 (2.0 mM) was used to start the reaction. The pH optimum for Mn^{2+} (0.5 mM) oxidation was determined in the same buffer using 0.2 mM H_2O_2 to start the reactions.

Enzyme kinetic constants (apparent K_m) were determined for fluoride, monochlorodimedone, and 2,6-dimethoxyphenol in fluoride-dependent reactions as well as for Mn^{2+} in Mn^{2+} oxidation using the spectrophotometric assays described above. The initial rate of the absorption decrease or increase was used for the calculation of the activity. The data for the enzyme kinetics were fitted to Michaelis−Menten kinetics, and the apparent K_m values were calculated using GraphPad (San Diego, CA) Prism.

Fluoride Binding to MnP-1. Fluoride or Mn^{2+} binding studies were performed as described previously (*19*) by recording the difference absorption spectra of MnP-1 in the presence and absence of fluoride or manganese. Both the reference and sample cuvettes contained 1 μM MnP-1 in 100 mM citrate/phosphate buffer at pH 3.4, 4.0, or 4.4. The spectra were recorded from 350 to 550 nm after stepwise addition of F^- or Mn^{2+} to the sample cuvette. The apparent dissociation constants (K_D) were calculated from plots of ΔA^{-1} (the difference between maximum and minimum absorptions) versus $[F^-]^{-1}$ or $[Mn^{2+}]^{-1}$.

The apparent dissociation constants (K_D) were calculated according to the following equation:

$$1/\Delta A = K_D/\Delta A_\infty \times 1/[S] + 1/\Delta A_\infty \quad (1)$$

where ΔA_∞ is the absorbance change for the complete formation of the MnP-1−fluoride or MnP-1−manganese adduct and [S] is the free F^- or Mn^{2+} concentration, which is assumed to be equal to the initial concentration because of the low enzyme concentration used.

The stoichiometry of F^- or Mn^{2+} binding to MnP-1 in the vicinity of the heme was calculated from the logarithmic form of the Hill equation shown below:

$$\log[\Delta A/(\Delta A_\infty - \Delta A)] = h \log[S] + \log K_D \quad (2)$$

where ΔA_∞ and K_D were calculated from eq 1.

For competitive inhibition of fluoride with respect to formation of the Mn^{3+}−malonate complex, tests were conducted as described previously (*20*) with minor modifications. Reactions were performed with 0.6 μg of MnP-1 from *B. adusta* strain Ud1 in 50 mM malonate buffer (pH 4.0) with Mn^{2+}, hydrogen peroxide, and fluoride concentrations given in the Results.

Identification of Products from MnP-1-Catalyzed Fluoride-Dependent Reactions. After precipitation of the MnP-1 enzyme by acidification and addition of CH_2Cl_2, the samples were centrifuged. Both the organic layer and the aqueous layer were subjected to LC−MS/MS analysis. Prior to LC−MS analysis of the CH_2Cl_2 layers, these samples were dried in an argon stream and redissolved in methanol.

The samples of the MCD and 2,6-dimethoxyphenol assays were analyzed using a Dionex 3000 HPLC system (Dionex, Idstein, Germany) equipped with a Phenomenex (Torrance,

Table 1: Fluoride-Dependent Monochlorodimedone (MCD) Consumption Activity of Manganese Peroxidases (MnPs) Purified from Different Fungal Species[a]

species	enzyme	MnP (units/mL)	MCD consumption rate[b] (units/mL)
B. adusta Ud1	MnP-1	183.2	7.4
C. dusenii b11	MnP	4.2	0.3
Phlebia spp. b19	MnP	14.3	1.4
P. eryngii DSM 9619	MnP-2	59.2	2.7

[a]One unit of MnP activity is defined as 1 μmol of Mn^{3+}−malonate complex formed per minute. One unit of F^--dependent MCD consumption is defined as 1 μmol of MCD consumed per minute. For experimental details for the enzyme assay, see Materials and Methods. [b]No significant conversion of MCD was observed in the absence of fluoride.

CA) Gemini HPLC column (250 mm × 2 mm, 5 μm) coupled with a Finnigan LTQ ESI-MS (Thermo Fisher Scientific, Egelbach, Germany) (mass range of 100−2000 Da). The compounds of the enzyme assays were separated by HPLC using gradient elution of solvent A (H_2O with 0.5% AcOH) and solvent B (MeCN with 0.5% AcOH) at a flow rate of 200 μL/min. After 100% A for 3 min, a linear gradient from 100% A to 100% B over 27 min was applied, followed by 100% B for 10 min. Identified reaction products were also analyzed by high-resolution mass spectrometry using an LTQ-Orbitrap (Thermo Fisher) at a resolution of 77000 or compared to an authentic standard.

RESULTS

Fluoride-Dependent Conversion of Organic Substrates Mediated by MnPs. During a screening for fungal haloperoxidases that might use fluoride as a halogen substrate, we observed a fluoride-dependent, Mn^{2+}-independent consumption of monochlorodimedone (MCD) mediated by a manganese peroxidase (designated MnP-1) that was purified from *B. adusta* strain Ud1. MCD consumption was monitored by the absorption decrease at 278 nm and by HPLC. The studies were extended to other MnPs and were found to occur only in the presence of fluoride (Table 1). This fluoride-dependent reaction was further investigated with respect to its substrates and kinetics.

We restricted our further studies on this reaction to MnP-1 of *B. adusta* strain Ud1. The substrate conversion and pH optimum were tested using different organic compounds (Table 2) in the absence of Mn^{2+} ions. An assay with Mn^{2+} ions as a reductant was used for comparison (Table 2). Except veratryl alcohol, which, under the conditions applied, has a high redox potential of 1.4 V (*21*), all other substrates tested were converted by MnP-1 in the presence of F^- and H_2O_2 (Table 2). These Mn^{2+}-independent activities indicated that in the presence of fluoride MnP-1 was able to convert different organic substrates. No significant substrate conversion was observed in the absence of either fluoride [shown in Figure 2 for MCD consumption (A) and 2,6-dimethoxyphenol oxidation (B)] or the enzyme. The apparent K_m values for 2,6-dimethoxyphenol (DMP) and MCD were between 0.1 and 1 mM for MnP-1 in the presence of 20 mM fluoride and 1 mM H_2O_2.

The pH optimum of the MnP-1-mediated fluoride-dependent consumption of organic substrates including MCD was determined to be ~3 (Table 2), whereas Mn(II) oxidation exhibited a pH optimum around 5.0 (Table 2; see also ref *22*). High concentrations of fluoride were required to support the reaction.

Table 2: Substrates Converted by and pH Optima of MnP-1 Purified from *B. adusta* Strain Ud1[a]

substrate	ion present	$[H_2O_2]$ (mM)	specific activity (units/mg)	pH optimum
ABTS (0.3 mM)	20 mM F^-	1.0	29.7	3.5
2,6-DMP (1.0 mM)	20 mM F^-	1.0	21.1	3.0
MCD (0.1 mM)	20 mM F^-	1.0	19.9	3.0−3.5
guaiacol (1.0 mM)	20 mM F^-	1.0	2.0	3.5
VA (4.0 mM)	20 mM F^-	1.0	0	−
Mn^{2+} (0.5 mM)	0.5 mM Mn^{2+}	0.2	259.2	4.5−5.5
2,6-DMP (1.0 mM)	0.5 mM Mn^{2+}	0.2	101.5	5.0

[a]For experimental details, see Materials and Methods.

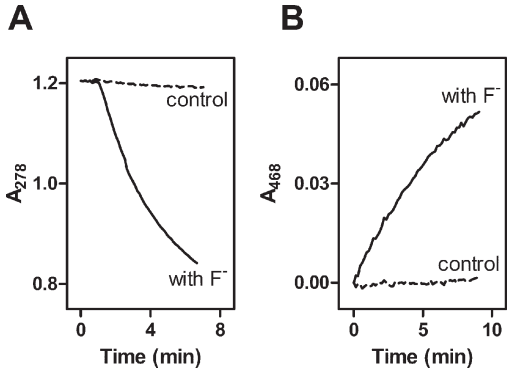

FIGURE 2: (A) Consumption of monochlorodimedone (MCD) and (B) oxidation of 2,6-dimethoxyphenol (DMP) in the presence and absence of fluoride. The reaction was conducted in 100 mM citrate/phosphate buffer (pH 2.8), with 0.1 mM MCD or 0.2 mM DMP, 1 mM H_2O_2, and 3 μg of MnP-1, in the presence or absence of 20 mM NaF.

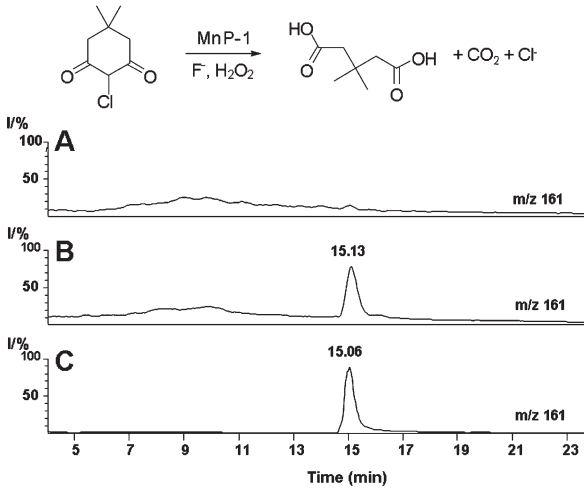

FIGURE 3: LC−MS analysis of the monochlorodimedone (MCD) conversion product in the presence of fluoride. (A) LC elution profile of an enzyme-free control assay. (B) LC elution profile of the reaction products of the fluoride-dependent MCD conversion. (C) LC elution profile of the standard compound 3,3-dimethylglutaric acid. The m/z values are shown for the $[M + H]^+$ ions. The reaction was conducted in 100 mM citrate/phosphate buffer (pH 2.8), with 0.1 mM MCD, 1 mM H_2O_2, and 20 mM NaF, in the presence or absence of 3 μg of MnP-1.

Oxidation of Monochlorodimedone and 2,6-Dimethoxyphenol by MnP-1 in the Presence of Fluoride. Under the experimental conditions applied, MCD and hydrogen peroxide were consumed in a stoichiometry of near 1:1 in the presence of 20

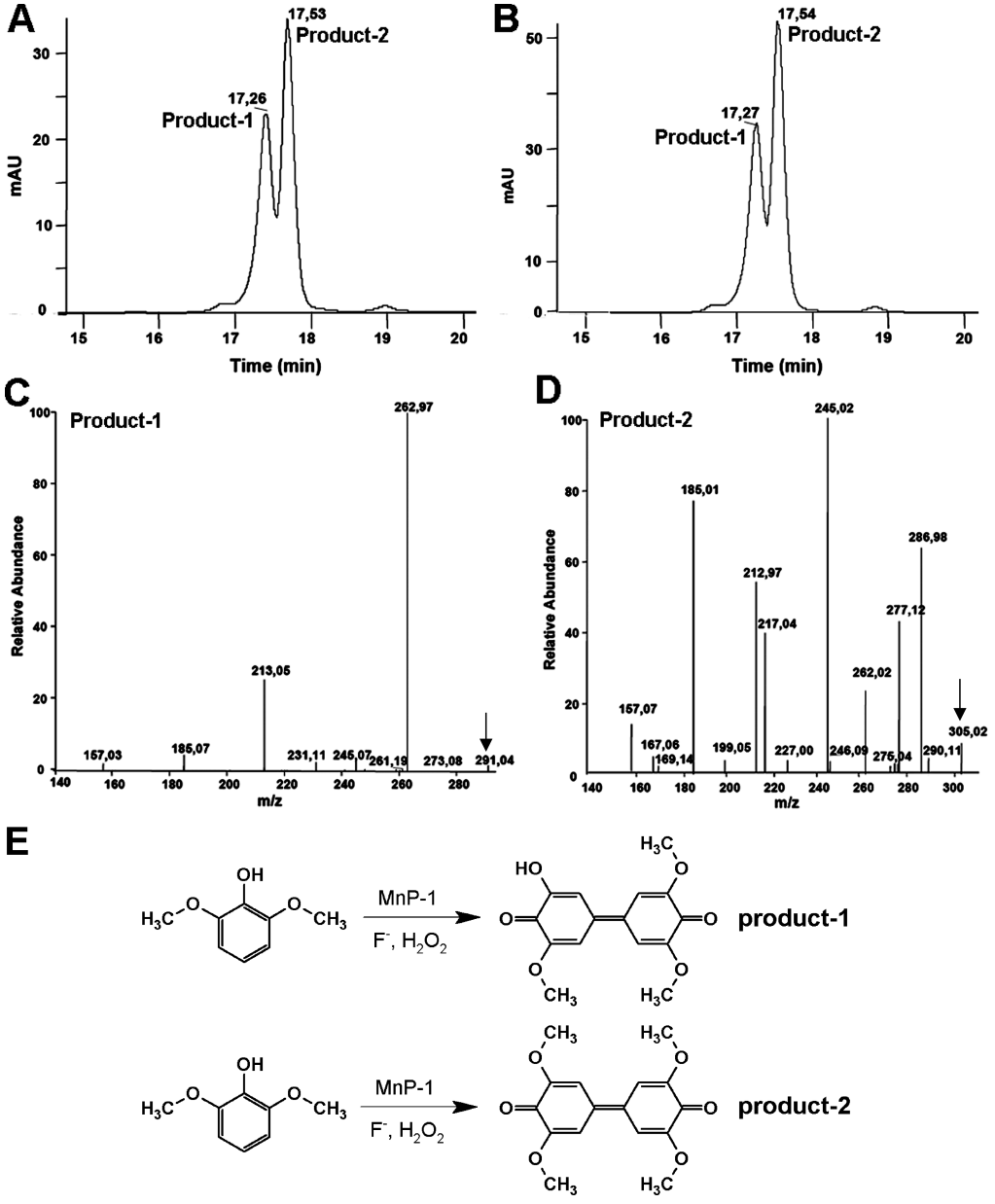

FIGURE 4: LC−MS analysis of 2,6-dimethoxyphenol (DMP) conversion products in the presence of F^- or Mn^{2+} ions. (A) LC elution profile in the presence of fluoride. (B) LC elution profile in the presence of Mn^{2+} ions. (C) ESI-MS/MS spectrum after fragmentation of the $[M + H]^+$ ion at m/z 305 of product-1 of the fluoride-dependent reaction. (D) ESI-MS/MS spectrum after fragmentation of the $[M + H]^+$ ion at m/z 291 of product-2 of the fluoride-dependent reaction. (E) Reaction equations of DMP oxidation. Arrows in panels C and D indicate the mass peak of product-1 and product-2, respectively. The assays were conducted in 100 mM citrate/phosphate buffer (pH 4.0), with 0.2 mM DMP, 0.1 mM H_2O_2, and 3 μg of MnP-1, in the presence of 20 mM NaF or 150 μM $MnCl_2$.

mM NaF (data not shown). MCD was not converted in the presence of Mn^{2+} ions (150 μM) or in the absence of F^- ions.

The product of the fluoride-dependent MCD conversion was identified by ESI-MS to be 3,3-dimethylglutaric acid. Its ESI-MS $[M + H]^+$ was 161; its ESI-MS/MS of 161 was 143 (100), and its ESI-MS^3 of 161 of 143 was 115 (100), 97 (4), and 73 (4). The retention time of the product was 15.1 min as determined by LC−MS, which was identical with that of an authentic standard of 3,3-dimethylglutaric acid (Figure 3).

To gain additional information about the fluoride-dependent catalysis, we used 2,6-dimethoxyphenol as a substrate in further studies. Formation of 3,3′,5,5′-tetramethoxy-4,4′-diphenoquinone is known to occur in the Mn^{2+}-dependent oxidation of DMP (*18*).

The reaction products of 2,6-dimethoxyphenol (DMP) conversion in the presence of fluoride were subjected to LC−MS analysis and compared to those formed in the presence of Mn^{2+} ions. The elution profile obtained by LC−MS analysis indicated that the same reaction products were formed from DMP by MnP-1 in the fluoride-dependent (Figure 4A) and manganese-dependent (Figure 4B) reactions.

The mass spectra of the reaction products (shown for the reaction with fluoride in Figure 4C,D) exhibited $[M + H]^+$ ions at m/z 291 and 305. The molecular masses of the two reaction products were accordingly calculated as 290 and 304, respectively. High-resolution mass spectrometry analysis of these reaction products suggested molecular formulas of $C_{15}H_{14}O_6$ and $C_{16}H_{16}O_6$, respectively, supporting the assumption that the major product (product-2 in Figure 4; t_R = 17.53 min) was a dimer of 2,6-dimethoxyphenol, whereas the minor product (product-1 in Figure 4; t_R = 17.26 min) with a molecular mass

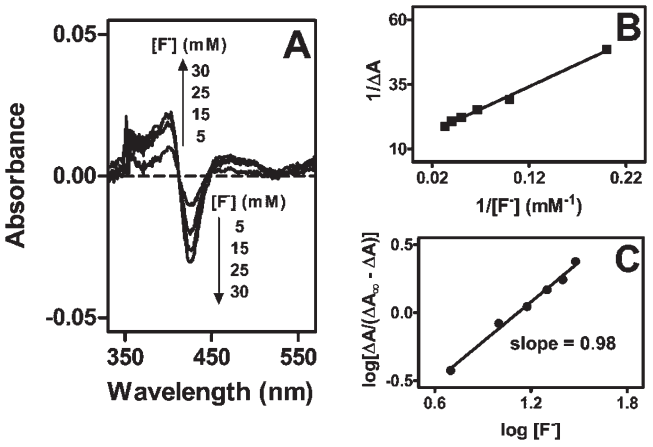

FIGURE 5: Fluoride binding to MnP-1 at pH 4.0. (A) Difference spectra of MnP-1 upon fluoride addition at the concentrations indicated. (B) Double-reciprocal plot of ΔA vs [S] for the calculation of the apparent dissociation constant (K_D) and ΔA_∞ from the slope and y intercept. (C) Hill plot for quantifying the stoichiometry of fluoride bound per MnP-1 heme.

Table 3: K_D Values of F^- and Mn^{2+} for Binding to MnP-1 at Different pH Values

	K_D (mM)		
ligand	pH 3.4	pH 4.0	pH 4.4
F^-	2.5	13.0	565.00
Mn^{2+}	> 30	0.5	0.03

of 290 was a dimer from which a methyl group was eliminated. The $[M + H]^+$ ion of product-1 measured with ESI-HR-MS was 291.08633 [calcd 291.08631 ($C_{15}H_{15}O_6$)]. ESI-HR-MS/MS of 291.09: 263.09161 (100), 245.08058 (2), 231.06534 (2), 213.05476 (27), 185.05948 (5), 157.06482 (2), 129.06979 (1). The $[M + H]^+$ ion of product-2 measured with ESI-HR-MS was 305.10199 [calcd 305.10196 ($C_{16}H_{17}O_6$)]. ESI-HR-MS/MS of 305.10: 287.09149 (51), 277.10696 (39), 262.08365 (21), 245.08086 (100), 213.05469 (53), 185.05968 (75), 157.06493 (17), 129.07008 (1).

On the basis of the high-resolution mass spectra and in accordance with the literature (*18*), the reaction products were identified as 3,3′,5,5′-tetramethoxy-4,4′-diphenoquinone and its demethylated product. The formation of DMP dimers as major reaction products and the absence of any fluorinated compound signals in the ^{19}F NMR spectrum (data not shown) clearly showed that fluoride was not incorporated into the substrate. Quantification of the reaction substrate and products by absorption spectroscopy indicated a DMP:product stoichiometry of 2:1, which is in accordance with a dimerization of the substrate (data not shown).

Binding of Fluoride to MnP-1. Earlier experiments with MnPs of *Phanerochaete chrysosporium* indicated a binding of fluoride to the heme enzyme, which caused a spectral change of the heme (*12*). Therefore, the differential absorption spectra of MnP-1 were recorded in the absence and presence of varying concentrations of F^- or Mn^{2+} (shown for fluoride at pH 4 in Figure 5A). Upon addition of fluoride, the absorption difference at 405 nm increased and at 425 nm decreased, indicating a binding of fluoride or HF close to the heme.

The apparent dissociation constants (K_D) and the maximal absorption difference (ΔA_∞) obtained upon titration of MnP-1 with the ions could be calculated from slope and intercept of the

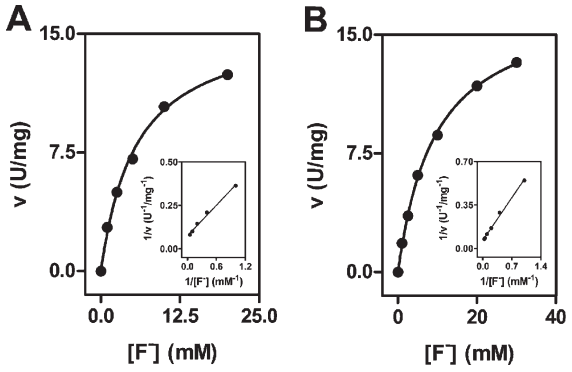

FIGURE 6: Reaction kinetics of monochlorodimedone (MCD) (A) or 2,6-dimethoxyphenol (DMP) (B) consumption at varying fluoride concentrations. The Lineweaver−Burk plots are shown as insets. The reactions were conducted in 100 mM citrate/phosphate buffer (pH 2.8) containing 0.6 μg of MnP-1 in the presence of 0.1 mM MCD or 1 mM DMP.

double-reciprocal plot of ΔA versus [S] (Figure 5B). The Hill plot of $\log[\Delta A/(\Delta A_\infty - \Delta A)]$ versus log[S] exhibited a straight line with slopes (h) of 0.98 (Figure 5C) and 0.97 (data not shown) for F^- and Mn^{2+}, respectively, indicating the binding of a single atom of F^- or Mn^{2+} to or close to the heme of the native enzyme.

The dissociation constant (K_D) for F^- was lower at lower pH (Table 3). At pH 3.4, no spectral change was observed at 30 mM Mn^{2+}, indicating a very high K_D value. The K_D values listed in Table 3 also indicate an affinity of Mn^{2+} higher than that of fluoride for the enzyme.

The rate of monochlorodimedone or 2,6-dimethoxyphenol conversion increased with an increase in fluoride concentration (Figure 6A,B). High fluoride concentrations (5.6 or 9.6 mM) were required to obtain half-maximal reaction velocity. This type of kinetics may be interpreted to indicate that fluoride binding to the enzyme is essential for catalysis.

The Lineweaver−Burk plots of formation of the Mn^{3+}−malonate complex with varying concentrations of Mn^{2+} and fluoride were linear and parallel, indicating that fluoride is an uncompetitive inhibitor of Mn^{2+} (data not shown); a K_i value of 32.5 mM was calculated from this experiment. The uncompetitive inhibition type indicates that fluoride and Mn^{2+} bind to different sites.

When formation of Mn^{3+} from Mn^{2+} was assessed with different concentrations of fluoride and H_2O_2, the Lineweaver−Burk plots were linear with a common ordinate intercept (Figure 7A), showing that fluoride was a competitive inhibitor for hydrogen peroxide in MnP-1-catalyzed Mn^{2+} oxidation; a K_i of 6.3 mM for fluoride was calculated from the replot of the slope (apparent K_m/V_{max}) versus [F^-] (Figure 7A, inset). Upon addition of increasing fluoride concentrations, the MnP activity decreased, until a constant Mn^{2+} oxidation rate was reached. Beyond a fluoride concentration of ~20 mM, no further decrease in the activity was observed, indicating a partially competitive inhibition type (Figure 7B). The result points to a concomitant binding of fluoride (or HF) and H_2O_2 to the enzyme (*23*).

To investigate the effect of Mn^{2+} on the fluoride-dependent reaction, monochlorodimedone (0.1 mM) was used as a substrate, because its conversion is strictly fluoride-dependent and manganese-independent. Mn^{2+} was found to severely inhibit the fluoride-dependent MCD conversion; with as little as 30 μM Mn^{2+}, the reaction rate decreased by 60% (data not shown). The inhibitory effect of Mn^{2+} on the fluoride-dependent MCD

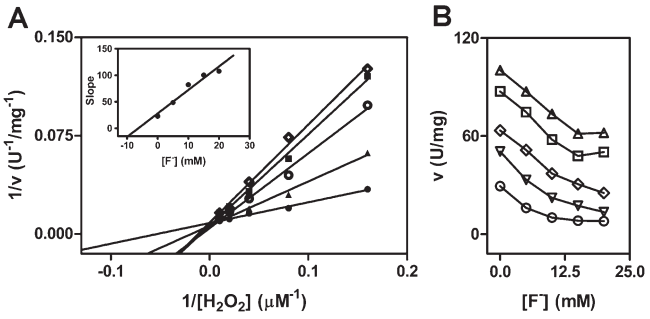

FIGURE 7: Reaction kinetics of Mn^{2+} oxidation at varying concentrations of fluoride and hydrogen peroxide. (A) Lineweaver−Burk plot of $1/v$ vs $1/[H_2O_2]$. The inset is a replot of the slope of the inverse plot vs $[F^-]$. Reaction mixtures contained 0.6 μg/mL MnP-1 of *B. adusta* strain Ud1 with varying H_2O_2 concentrations as indicated. NaF concentrations of 0 (●), 5 (▲), 10 (○), 15 (■), and 20 mM (◇) were used. (B) Effect of $[F^-]$ on the Mn^{2+} oxidation rate. H_2O_2 concentrations of 6.25 (○), 12.5 (▽), 25 (◇), 50 (□), and 100 μM (△).

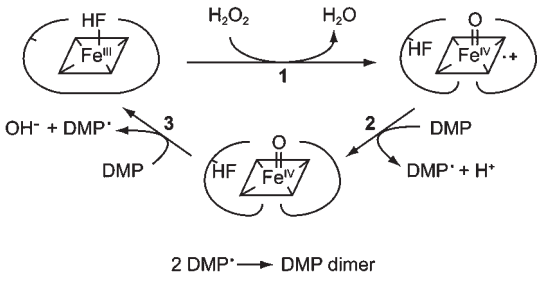

FIGURE 8: Proposed mechanism of the fluoride-dependent 2,6-dimethoxyphenol (DMP) oxidation mediated by manganese peroxidase in the absence of Mn^{2+}. HF represents either the fluoride anion or the corresponding acid.

conversion might be explained by the competition of Mn^{2+} and MCD as electron donors for H_2O_2 reduction.

DISCUSSION

In screening for fungal halogenating peroxidases, we used the monochlorodimedone (MCD) assay. The MCD assay is generally applied for haloperoxidases (*24*). Using this assay, we found a fluoride-dependent MCD conversion which was not associated with fluorination. This finding leads to a critical view of the application of the MCD assay for haloperoxidases. As suggested previously (*25*), a negative control without halide ion should always be applied to minimize the false positive reactions caused by unspecific oxidation of MCD by the peroxidase. However, our study shows that this control might not provide unambiguous proof for a halogenation reaction. A monochlorodimedone conversion by a heme protein of the cytochrome *c* family was reported previously (*25*); however, no reaction products were identified. The molecular mass of the MCD conversion product of the cytochrome *c*-type protein (*25*) was the same as that determined in our study; hence, it is likely that the reaction products were the same for both enzymes. The oxidation catalyzed by MnP-1 leads to the breakdown of MCD that undergoes ring opening, followed by oxidative loss of one C atom to finally yield 3,3-dimethylglutaric acid.

Fluoride was found to support oxidation of organic substrates catalyzed by manganese peroxidases (MnPs) in the absence of Mn^{2+} at acidic pH values. Because the fluoride-dependent, manganese-independent oxidation of organic compounds was observed for different fungal MnPs, it may be a common feature of these enzymes. This finding is in contrast to the previously assumed strict manganese dependence of manganese peroxidase activities, including the oxidation of organic compounds.

The formerly reported oxidation of phenolic compounds by compound I of MnP in the absence of Mn^{2+} ions (*5*, *26*) is a dead-end reaction leading to the formation of compound II (see Figure 1), the reduction of which strictly requires Mn^{2+} ions. The fluoride-dependent reaction described in this communication is mediated in a complete reaction cycle with catalytic rather than stoichiometric amounts of enzyme. The low pH optimum of the MnP-mediated oxidation of phenolic compounds or monochlorodimedone in the presence of fluoride is in accordance with earlier findings that lignin peroxidases (LiPs) and versatile peroxidases (VPs) generally exhibit a low pH optimum for the oxidation of organic compounds (*27*, *28*); the pH optimum of MnPs for the oxidation of Mn^{2+} ions is higher (*22*). This indicates that the reaction mechanism of the MnP-catalyzed fluoride-dependent oxidation reaction may be similar to that of LiP and VP. MnP-mediated fluorination could be excluded by LC−MS and ^{19}F NMR analysis of the reaction products (data not shown). 2,6-dimethoxyphenol was converted to 3,3′,5,5′-tetramethoxy-4,4′-diphenoquinone and the monodemethylated 3-hydroxy-3′,5,5′-trimethoxy-4,4′-diphenoquinone. The formation of 3,3′,5,5′-tetramethoxy-4,4′-diphenoquinone has been observed previously for Mn^{2+}-dependent DMP conversion (*18*). O-Demethylation was described for 1,2,4,5-tetramethoxybenzene oxidation by lignin peroxidase (*29*) and by P450 enzymes (*30*, *31*). To the best of our knowledge, O-demethylation has not been reported so far to be mediated by manganese peroxidases, even in the presence of Mn^{2+} ions.

Although fluoride was not a substrate for the enzyme, the presence of fluoride was obligatory and the velocity of the fluoride-dependent reactions increased with an increase in fluoride concentration. The difference spectroscopy showed that fluoride binds to MnP-1 of *B. adusta* strain Ud1 in the heme pocket with a stoichiometric ratio of 1:1 at acidic pH values. As reported previously, fluoride or HF can coordinate to the heme iron of heme-containing peroxidases, e.g., horseradish peroxidase and cytochrome *c* peroxidase, as a sixth ligand to form a high-spin ferric hexacoordinate species if the sixth coordination position of the heme iron is vacant or occupied by a weak field ligand such as water (*32*).

The oxidation of organic substrates in the presence of fluoride and in the absence of manganese is depicted in a simplified scheme (Figure 8). This proposed reaction mechanism is a modification of the normal reaction cycle of manganese peroxidase for Mn^{2+} oxidation (see Figure 1). According to this scheme, HF or fluoride binds as a distal ligand to the heme ferric iron. The finding that fluoride was found to be a partially competitive inhibitor for hydrogen peroxide binding in Mn^{2+} oxidation indicates that fluoride and H_2O_2 bind to the same site, i.e., the heme iron. It is not feasible that both fluoride and hydrogen peroxide bind simultaneously to the iron. Because for the oxidation of organic compounds binding of H_2O_2 to the heme is required, fluoride has to move elsewhere to exert its effect (reaction 1 in Figure 8). An alternative fluoride binding site has also been proposed to be present in the lignin peroxidase of *Ph. chrysosporium* (*19*) and in haloperoxidases (*33*). Under these conditions, the organic substrates are oxidized. In the further reaction cycle (reactions 2 and 3 in Figure 8), the heme is reduced in two one-electron transfer steps that have been identifed for all heme peroxidases. The conversion of organic substrates by the

fluoride-binding manganese peroxidase can therefore only be explained by a conformational change of the peptide chain.

Two alternative mechanisms for the transfer of electrons from the substrate to the heme as a result of fluoride binding can be proposed. Either a distal long-range electron transfer pathway (LRET) for the oxidation of organic compounds is opened, or the conformation of the protein is changed so that aromatic compounds have access to the heme pocket and can directly be oxidized. In addition to the common proximal LRET, the presence of a putative distal LRET in different versatile peroxidases has been proposed (*7*, *8*). In the versatile peroxidase PS1 of *P. eryngii*, amino acids H82, A83, and N84 have been suggested to be part of this LRET. Similar amino acids are also present at the same position in some manganese peroxidases [e.g., those of *Trametes versicolor*, *Ceriporiopsis rivulosa*, and *Pleurotus ostreatus* (GenBank accession numbers AAT90348.1, BAB03464.1, ABB83813.1, and ACM47219.1)]. Therefore, the involvement of a distal LRET opened by fluoride binding to MnP is feasible. According to the alternative hypothesis, the heme pocket might by extended by fluoride binding to allow access of the substrates via the main heme access channel. For the horseradish peroxidase, this is the general reaction mechanism (*34*−*36*). For versatile peroxidases, this option has been indirectly shown by site-directed mutagenesis (*8*). In the absence of fluoride, organic substrates cannot reach the active site of manganese peroxidase. In the case of LiP, it has been shown that the main heme access channel is too small to allow access even for small organic substrates (*37*). It is, however, feasible that the heme access channel is extended by fluoride binding to the protein. In principle, fluoride binding to heme peroxidases can cause conformational changes of the peptide chain (*38*, *39*). However, this has only been reported so far for fluoride binding to the heme iron.

Once the conformational change is achieved by fluoride binding, organic compounds such as DMP may be oxidized either in the heme pocket or externally via the distal LRET (Figure 8, reactions 2 and 3). The radicals formed from the organic substrates may then form dimers as observed for DMP or undergo further nonenzymatic reactions, which could be the case for MCD.

Because fluoride binding occurs at the distal site of the heme, it is believed that the alternative fluoride binding site is also distal. Otherwise, the fluoride would have to move from the distal to the proximal site of the heme. Therefore, if the hypothesis of the distal LRET activation by fluoride proves to be valid, the transfer of electrons from the aromatic compounds should also occur at the distal site. Proximal long-range electron transfer pathways are known to occur in other peroxidases such as LiPs or VPs and were suggested to play a major role in the oxidation of organic substrates (*7*, *8*). For MnPs, a proximal LRET for the oxidation of organic substrates appears unlikely, since the proximal LRET involves a tryptophan residue that is not present in manganese peroxidases (*6*). Further experiments are required to elucidate the reaction mechanism of this unusual oxidation of organic compounds mediated by manganese peroxidase in the presence of fluoride and in the absence of manganese.

The reason for and the physiological impact of the fluoride-dependent electron transfer from organic substrates to the heme are so far not clear. In natural environments such as soil, the fluoride concentration is low (e.g., < 0.2 ppm soluble fluoride in agricultural soil) (*40*). However, the possibility that the binding of compounds other than fluoride, which are more abundant and more readily available in nature, might exert an influence similar to that of fluoride under laboratory conditions cannot be excluded.

ACKNOWLEDGMENT

We express our gratitude to Kerstin Ploss (Department of Bioorganic Chemistry, Max Planck Institute for Chemical Ecology) for technical assistance.

SUPPORTING INFORMATION AVAILABLE

Additional experimental observations. This material is available free of charge via the Internet at http://pubs.acs.org.

REFERENCES

1. Glenn, J. K., Akileswaran, L., and Gold, M. H. (1986) Mn(II) oxidation is the principal function of the extracellular Mn-peroxidase from *Phanerochaete chrysosporium*. *Arch. Biochem. Biophys. 251*, 688–696.
2. Sundaramoorthy, M., Kishi, K., Gold, M. H., and Poulos, T. L. (1994) The crystal structure of manganese peroxidase from *Phanerochaete chrysosporium* at 2.06-Å resolution. *J. Biol. Chem. 269*, 32759–32767.
3. Kishi, K., Hildebrand, D. P., Kusters-van Someren, M., Gettemy, J., Mauk, A. G., and Gold, M. H. (1997) Site-directed mutations at phenylalanine-190 of manganese peroxidase: Effects on stability, function, and coordination. *Biochemistry 36*, 4268–4277.
4. Petruccioli, M., Frasconi, M., Quaratino, D., Covino, S., Favero, G., Mazzei, F., Federici, F., and D'Annibale, A. (2009) Kinetic and redox properties of MnP II, a major manganese peroxidase isoenzyme from *Panus tigrinus* CBS 577.79. *J. Biol. Inorg. Chem. 14*, 1–11.
5. Wariishi, H., Akileswaran, L., and Gold, M. H. (1988) Manganese peroxidase from the basidiomycete *Phanerochaete chrysosporium*: Spectral characterization of the oxidized states and the catalytic cycle. *Biochemistry 27*, 5365–5370.
6. Timofeevski, S. L., Nie, G., Reading, N. S., and Aust, S. D. (1999) Addition of veratryl alcohol oxidase activity to manganese peroxidase by site-directed mutagenesis. *Biochem. Biophys. Res. Commun. 256*, 500–504.
7. Pérez-Boada, M., Ruiz-Duerias, F. J., Pogni, R., Basosi, R., Choinowski, T., Martinez, M. J., Piontek, K., and Martinez, A. T. (2005) Versatile peroxidase oxidation of high redox potential aromatic compounds: Site-directed mutagenesis, spectroscopic and crystallographic investigation of three long-range electron transfer pathways. *J. Mol. Biol. 354*, 385–402.
8. Ruiz-Duenas, F. J., Morales, M., Garcia, E., Miki, Y., Martinez, M. J., and Martinez, A. T. (2009) Substrate oxidation sites in versatile peroxidase and other basidiomycete peroxidases. *J. Exp. Bot. 60*, 441–452.
9. Ferguson-Miller, S., Babcock, G. T., and Yocum, C. (2006) Photosynthesis and respiration. In Biological inorganic chemistry: Structure and reactivity (Gray, H. B., Stiefel, E. I., Valentine, J. S., and Bertini, I., Eds.) pp 278−301, University Science Books, New York.
10. Coll, R. J., and Murphy, A. J. (1992) Fluoride-inhibited calcium ATPase of sarcoplasmic reticulum. Magnesium and fluoride stoichiometry. *J. Biol. Chem. 267*, 21584–21587.
11. Vanden Abbeele, A., Courtois, P., and Pourtois, M. (1995) The influence of different fluoride salts on fluoride-mediated inhibition of peroxidase activity in human saliva. *Arch. Oral Biol. 40*, 695–698.
12. Sheng, D., and Gold, M. H. (1997) Haloperoxidase activity of manganese peroxidase from *Phanerochaete chrysosporium*. *Arch. Biochem. Biophys. 345*, 126–134.
13. Neri, F., Kok, D., Miller, M. A., and Smulevich, G. (1997) Fluoride binding in hemoproteins: The importance of the distal cavity structure. *Biochemistry 36*, 8947–8953.
14. Edwards, S. L., and Poulos, T. L. (1990) Ligand binding and structural pertubations in cytochrome c peroxidase: A crystallographic study. *J. Biol. Chem. 265*, 2588–2595.
15. Hofrichter, M., and Fritsche, W. (1997) Depolymerization of low-rank coal by extracellular fungal enzyme systems. II. The ligninolytic enzymes of the coal-humic-acid-depolymerizing fungus *Nematoloma frowardii* b19. *Appl. Microbiol. Biotechnol. 47*, 419–424.
16. Ullrich, R., Nuske, J., Scheibner, K., Spantzel, J., and Hofrichter, M. (2004) Novel haloperoxidase from the agaric basidiomycete *Agrocybe aegerita* oxidizes aryl alcohols and aldehydes. *Appl. Environ. Microbiol. 70*, 4575–4581.

17. Bradford, M. M. (1976) A rapid and sensitive method for the quantitation of microgram quantities of protein utilizing the principle of protein-dye binding. *Anal. Biochem. 72*, 248–254.
18. Wariishi, H., Valli, K., and Gold, M. H. (1992) Manganese(II) oxidation by manganese peroxidase from the basidiomycete *Phanerochaete chrysosporium*. Kinetic mechanism and role of chelators. *J. Biol. Chem. 267*, 23688–23695.
19. Renganathan, V., Miki, K., and Gold, M. H. (1987) Haloperoxidase reactions catalyzed by lignin peroxidase, an extracellular enzyme from the basidiomycete *Phanerochaete chrysosporium*. *Biochemistry 26*, 5127–5132.
20. Youngs, H. L., Sundaramoorthy, M., and Gold, M. H. (2000) Effects of cadmium on manganese peroxidase: Competitive inhibition of Mn-II oxidation and thermal stabilization of the enzyme. *Eur. J. Biochem. 267*, 1761–1769.
21. Branchi, B., Galli, C., and Gentili, P. (2005) Kinetics of oxidation of benzyl alcohols by the dication and radical cation of ABTS. Comparison with laccase-ABTS oxidations: An apparent paradox. *Org. Biomol. Chem. 3*, 2604–2614.
22. Wariishi, H., Dunford, H. B., MacDonald, I. D., and Gold, M. H. (1989) Manganese peroxidase from the lignin-degrading basidiomycete *Phanerochaete chrysosporium*. Transient state kinetics and reaction mechanism. *J. Biol. Chem. 264*, 3335–3340.
23. Dixon, M., and Webb, E. C. (1979) Enzymes, 3rd ed., Academic Press, New York.
24. Hager, L. P., Morris, D. R., Brown, F. S., and Eberwein, H. (1966) Chloroperoxidase. II. Utilization of halogen anions. *J. Biol. Chem. 241*, 1769–1777.
25. Wagner, C., Molitor, I. M., and Koenig, G. M. (2008) Critical view on the monochlorodimedone assay utilized to detect haloperoxidase activity. *Phytochemistry 69*, 323–332.
26. Whitwam, R. E., Brown, K. R., Musick, M., Natan, M. J., and Tien, M. (1997) Mutagenesis of the Mn^{2+}-binding site of manganese peroxidase affects oxidation of Mn^{2+} by both compound I and compound II. *Biochemistry 36*, 9766–9773.
27. ten Have, R., Hartmans, S., Teunissen, P. J. M., and Field, J. A. (1998) Purification and characterization of two lignin peroxidase isozymes produced by *Bjerkandera* sp. strain BOS55. *FEBS Lett. 422*, 391–394.
28. Martinez, M. J., Ruiz-Duenas, F. J., Guillen, F., and Martinez, A. T. (1996) Purification and catalytic properties of two manganese peroxidase isoenzymes from *Pleurotus eryngii*. *Eur. J. Biochem. 237*, 424–432.
29. Kersten, P. J., Kalyanaraman, B., Kenneth, E. H., and Reinhammar, B. (1990) Comparison of lignin peroxidase, horseradish peroxidase and laccase in the oxidation of methoxybenzenes. *Biochem. J. 268*, 475–480.
30. Ibrahim, A. R. S., Galal, A. M., Ahmed, M. S., and Mossa, G. S. (2003) *O*-Demethylation and sulfation of 7-methoxylated flavanones by *Cunninghamella elegans*. *Chem. Pharm. Bull. 51*, 203–206.
31. Kinne, M., Poraj-Kobielska, M., Ralph, S. A., Ullrich, R., Hofrichter, M., and Hammel, K. E. (2009) Oxidative cleavage of diverse ethers by an extracellular fungal peroxygenase. *J. Biol. Chem. 284*, 29343–29349.
32. Mino, Y., Wariishi, H., Blackburn, N. J., Loehr, T. M., and Gold, M. H. (1988) Spectral characterization of manganese peroxidase, an extracellular heme enzyme from the lignin-degrading basidiomycete, *Phanerochaete chrysosporium*. *J. Biol. Chem. 263*, 7029–7036.
33. Thomas, J. A., Morris, D. R., and Hager, L. P. (1970) Chloroperoxidase. VIII. Formation of peroxide and halide complexes and their relation to the mechanism of the halogenation reaction. *J. Biol. Chem. 245*, 3135–3142.
34. Kare Meno, S. J., Smith, A. T., Henriksen, A., and Gajhede, M. (2002) Structural analysis of the two horseradish peroxidase catalytic residue variants H42E and R38S/H42E: Implication for the catalytic cycle. *Acta Crystallogr. D58*, 1803–1812.
35. Heering, H. A., Smith, A. T., and Smulevich, G. (2002) Spectroscopic characterisation of mutations at the Phe^{41} position in the distal haem pocket of horseradish peroxidase C: Structural and functional consequences. *Biochem. J. 363*, 571–579.
36. Smith, A. T., and Veitch, N. T. (1998) Substrate binding and catalysis in haem peroxidases. *Curr. Opin. Chem. Biol. 2*, 269–278.
37. Gerini, M. F., Roccatano, D., Baciochi, E., and Di Nola, A. (2003) Molecular dynamics simulations of lignin peroxidase in solution. *Biophys. J. 84*, 3883–3893.
38. Huang, Y. P., and Kassner, R. J. (1981) Fluoride binding to the cytochrome c ferric heme octapeptide. A model for anion binding to the active site of high spin ferric heme proteins. *J. Biol. Chem. 256*, 5327–5331.
39. Edwards, S. L., and Poulos, T. L. (1990) Ligand binding and structural perturbations in cytochrome c peroxidase. A crystallographic study. *J. Biol. Chem. 265*, 2588–2595.
40. Larsen, S., and Widdowson, A. E. (1971) Soil fluorine. *Eur. J. Soil Sci. 22*, 210–221.